Figure S1. Vascular density in the WT retina at P30.

(A) P30 whole retina flat mount from a WT (C57Bl/6) retina stained with GS-lectin (GSL). The GSL signal is color-coded by depth as in Figure 1, with the vitreal surface in blue, the IPL in green, and the OPL in red. Scale bar, 100 μm. (B) Quantification of vascular density as in Figure 1B-D. Each symbol is the quantification from one 500 μm x 500 μm area.

Figure S2. Incomplete recombination in early postnatal retinal astrocytes by the Gutmann *Gfap-Cre* line.

(A,B) Flat mount from *Gfap-Cre* (Gutmann); *R26-LSL-mtdT-2A-H2B-GFP* retinas imaged at the vitreal surface and showing the localization of Pax2 (red) and H2B-GFP (green) at P5 in (A). In (A), the optic disc is at the left of each image, and the peripheral edge of the retina is at the far right. Higher magnification images are shown at P4 for both the central (vascularized) and peripheral (nonvascularized) regions of retina (B). Scale bar in (A) 250 μm. Scale bar in (B) 50 μm.

Figure S3. Highly efficient *Cre*-mediated recombination in nearly all retinal cells by the *Six3-Cre* line.

Lower (left) and higher (right) exposures of the same retina section from a *Six3-Cre*;*Vegf*$^{fl/+}$;*R26-LSL-mtdT-2A-H2B-GFP* mouse stained for the H2B-GFP reporter to identify cells that have undergone *Cre*-mediated recombination, with GSL to identify blood vessels, and with DAPI. The lower exposure (left) shows that Muller glia, which have their cell bodies in the center of the INL (arrows in left image), and astrocytes, located at the vitreal face of the retina (arrowheads in left image), express high levels of the H2B-GFP reporter, whereas other retinal cells express H2B-GFP at lower levels. The higher exposure (right) shows that nearly every neuronal and glial nucleus contains H2B-GFP, whereas EC nuclei are H2B-GFP negative (arrows in right image). Scale bar, 100 μm.

Figure S4. Loss of astrocyte-derived and neural retina-derived VEGF does not alter astrocyte expression of PDGFRα.

Flat mounts of WT, *Six3-Cre*;*Vegf*$^{fl/fl}$, and *Gfap-Cre*;*Vegf*$^{fl/fl}$ retinas at P4, immunostained for astrocytes (GFAP and Pax2) and ECs (GSL). The optic disc is at the left of each image, and the peripheral edge of the retina is at the far right. Scale bar is 250 μm.

Figure S5. Normal patterns of expression for transcription factor markers in the developing hippocampus and cerebral cortex in *Gfap-Cre*;*Vegf*$^{fl/fl}$ mice.

Coronal sections at E17 of a phenotypically WT *Gfap-Cre*;*Vegf*$^{fl/+}$ brain (left) and a *Gfap-Cre*;*Vegf*$^{fl/fl}$ brain (right), stained for (i) Prox1, (ii) Ctip2, and (iii) Tbr1 and GSL. Prox1 is a marker for dentate gyrus progenitors; Ctip2 is a marker for cerebral cortical and striatal neurons, and Tbr1 is a marker for cerebral cortical neurons. The *Gfap-Cre*;*Vegf*$^{fl/fl}$ dorsal cortex is thin and hypovascular (arrows in lower right image), but the patterns of Prox1, Ctip2, and Tbr1 accumulation are unaltered. Scale bar, 500 μm.

Figure S6. Combined loss of *Hif1α* and *Hif2α* in radial glia and ventricular cells (in *Gfap-Cre*;*Hif1α*$^{fl/-}$;*Hif2α*$^{fl/-}$ mice) leads to hypovascularization and hypoplasia of the cerebral cortex.

(A) Top, dorsal views of P14 brains. In the phenotypically WT *Hif1α*$^{fl/-}$;*Hif2α*$^{fl/+}$ brain, the cerebral cortices cover most of the colliculus. In the *Gfap-Cre*;*Hif1α*$^{fl/-}$;*Hif2α*$^{fl/-}$ brain (right) the cortex is hypoplastic and the colliculus is partially exposed. Scale bar, 5 mm. Middle, coronal sections of P18 brains stained with GSL shows grossly normal anatomy and vascularization in the *Gfap-Cre*;*Hif1α*$^{fl/-}$;*Hif2α*$^{fl/-}$ brain. The boxed regions marked 'a' and 'b', are enlarged in the bottom pair of images. Scale bar for full brain sections, 1 mm. Scale bar for enlarged images, 200 μm. (B) Quantification of vascular density in dorsomedial cerebral cortex at P18 in phenotypically WT littermate control and in *Gfap-Cre*;*Hif1α*$^{fl/-}$;*Hif2α*$^{fl/-}$ mouse. Each symbol represents the quantification from one 500 μm x 500 μm square area. Eight different cortical areas from multiple 200 μm thick sections were quantified. (C) Quantification of body weights during the first 3-6 weeks of postnatal life in phenotypically WT controls (*Hif1α*$^{fl/-}$;*Hif2α*$^{fl/+}$ and *Hif1α*$^{fl/-}$;*Hif2α*$^{fl/-}$) and their *Gfap-Cre*;*Hif1α*$^{fl/-}$;*Hif2α*$^{fl/-}$ littermates. *Gfap-Cre*;*Hif1α*$^{fl/-}$;*Hif2α*$^{fl/-}$ mice exhibit minimally reduced weight gain that is not statistically significant at any of the ages tested.

Figure S7. Two sub-lines of the original Genentech *Vegf*^{fl} mouse line: line 1 lacks the 3' *loxP* site and line 2 has both 5' and 3' *loxP* sites.

(A) Schematic representation of the *Vegf*^{fl} allele. The identification number and nucleotide coordinates of *Vegf* exons 3-5 (mouse genome GRCm38/mm10) are: Exon 3, ENSMUSE00000136598, Chr17:46,025,543-46,025,347; exon 4, ENSMUSE00000225014, chr17:46,024,520-46,024,444; exon 5, ENSMUSE00001243553, Chr17:46,024,094-46,024,065. The mouse genome GRCm38/mm10 sequence is numbered on the antisense strand. The locations of the genotyping primers are marked with red arrowheads and the two *loxP* sites, 5' *loxP* at Chr17:46,026,234 and 3' *loxP* at Chr17: 46,024,767, are marked by red lines. (B) PCR products from genomic DNA extracted from tail clips were resolved by agarose gel electrophoresis and stained with ethidium bromide. Mice from *Vegf*^{fl} lines 1 and 2 contain the 5' *loxP* site (upper band, first set of PCR products). Only mice from line 2 contain the 3' *loxP* site (upper band, second set of PCR products). In the presence of *Gfap-Cre*, which recombines in the skin, the *Vegf* null allele is generated in line 2 but not in line 1 (third set of PCR products). The fourth set of PCR products shows the presence of *Cre* sequences from *Gfap-Cre*.

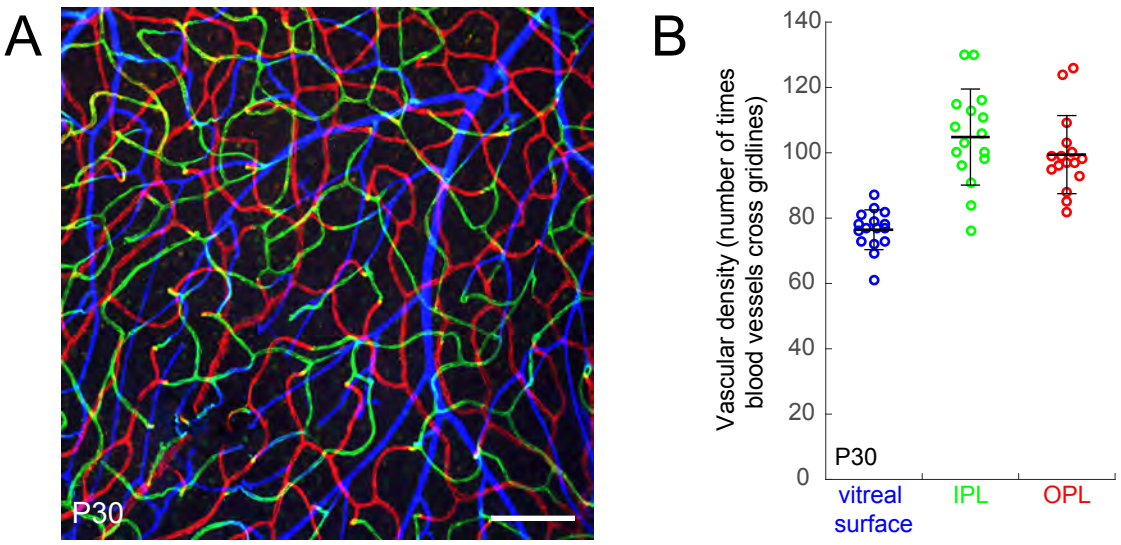

Rattner et al. Figure S1

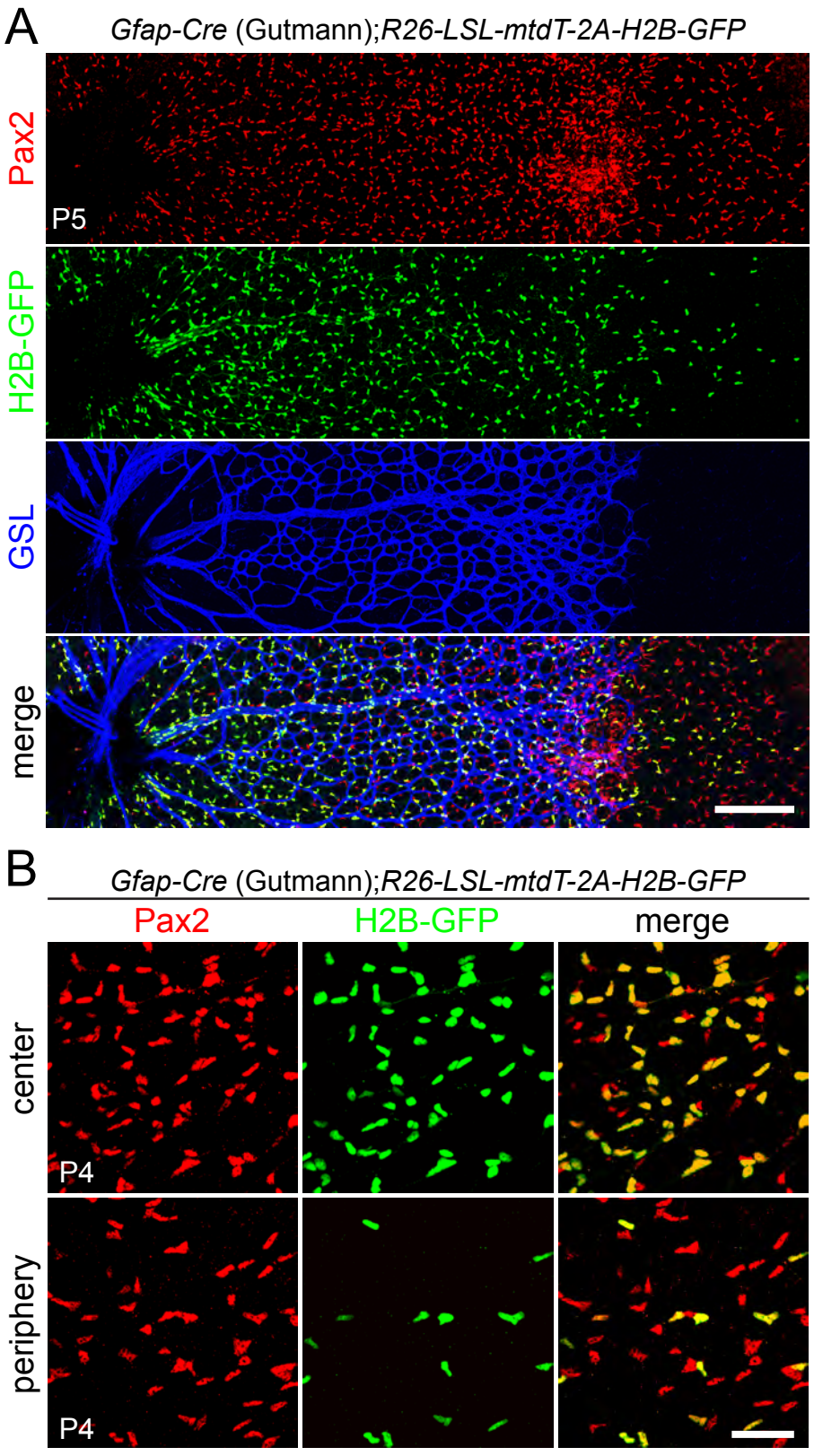

Rattner et al. Figure S2

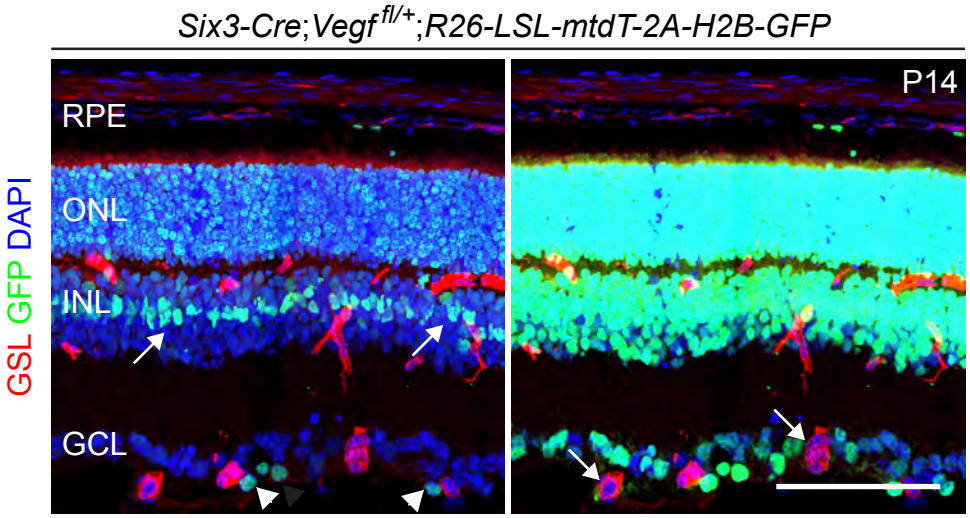

Rattner et al. Figure S3

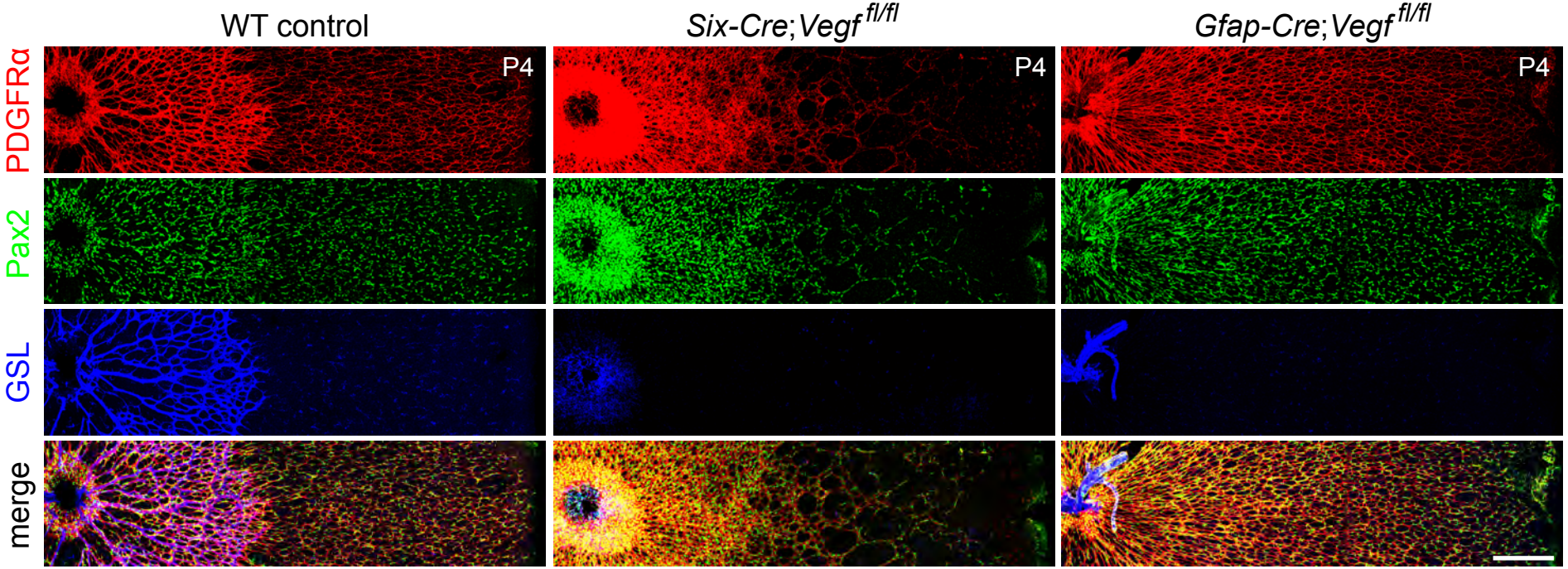

Rattner et al. Figure S4

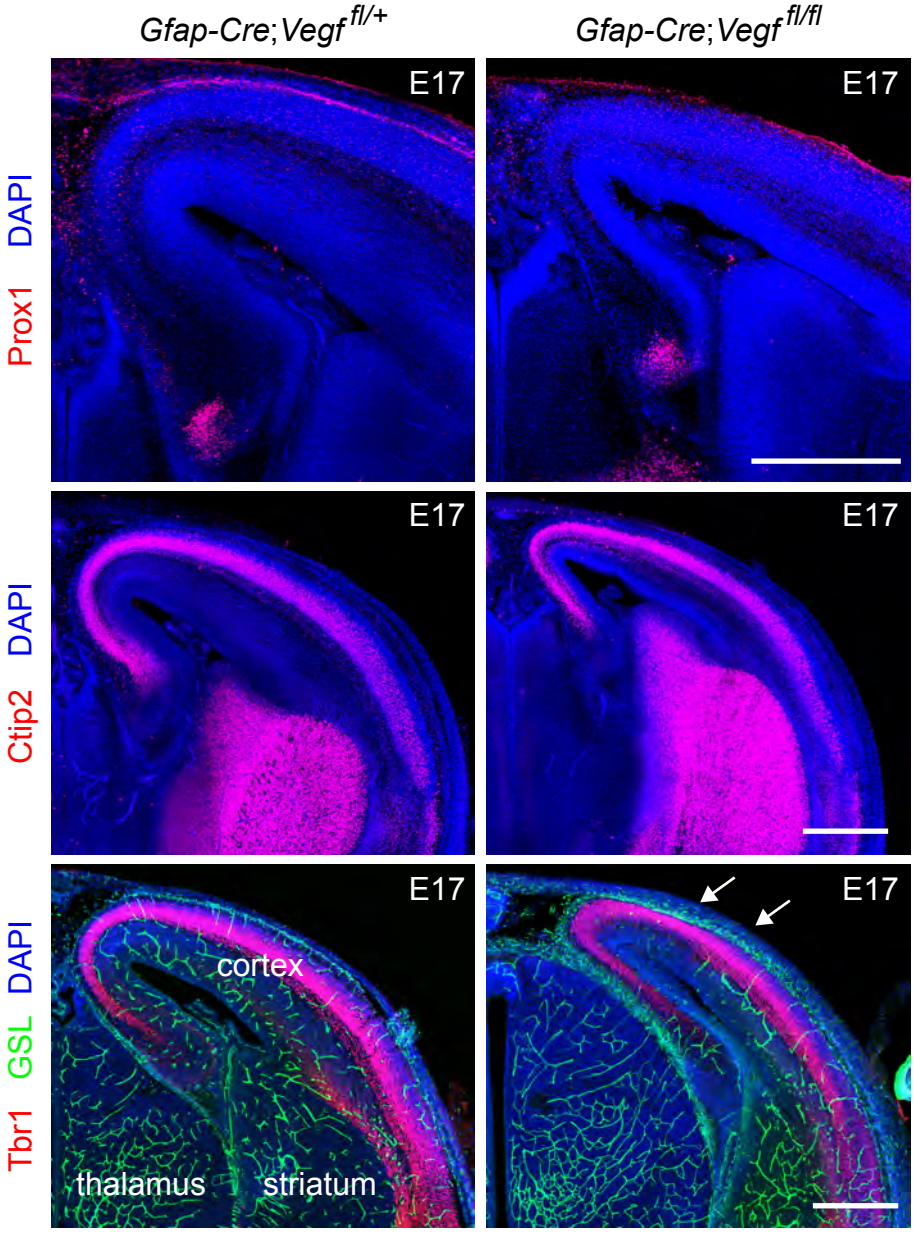

Rattner et al. Figure S5

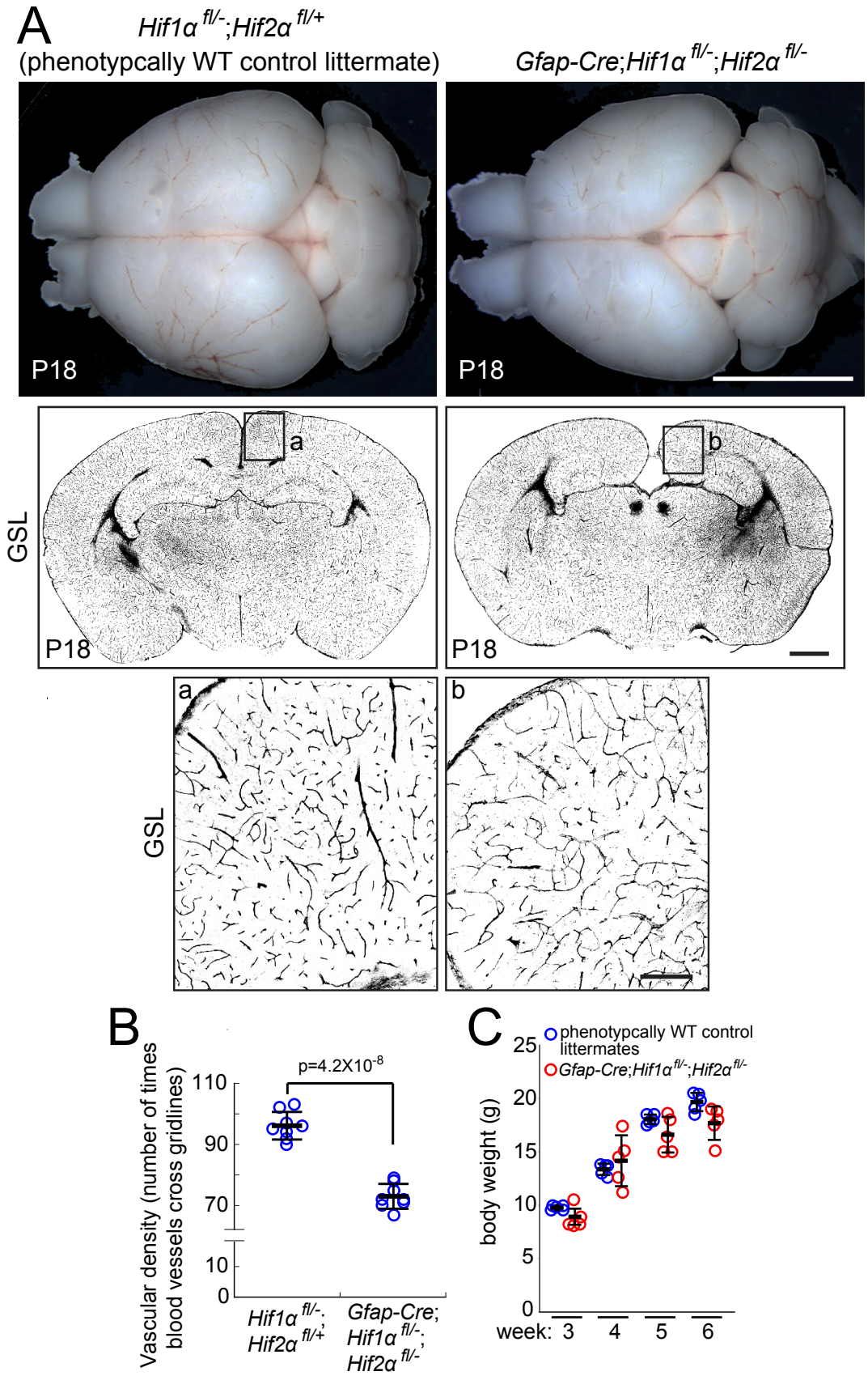

Rattner et al. Figure S6

A

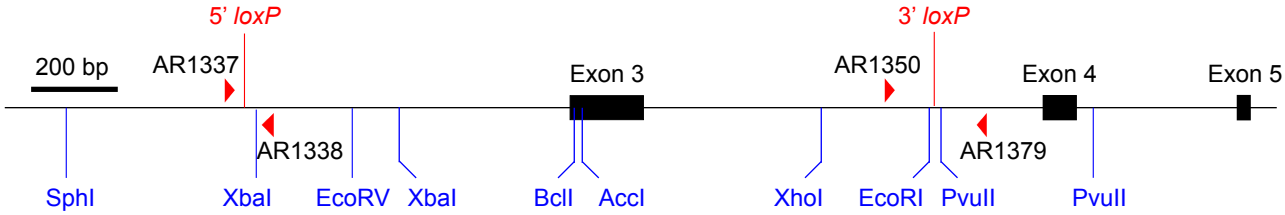

B

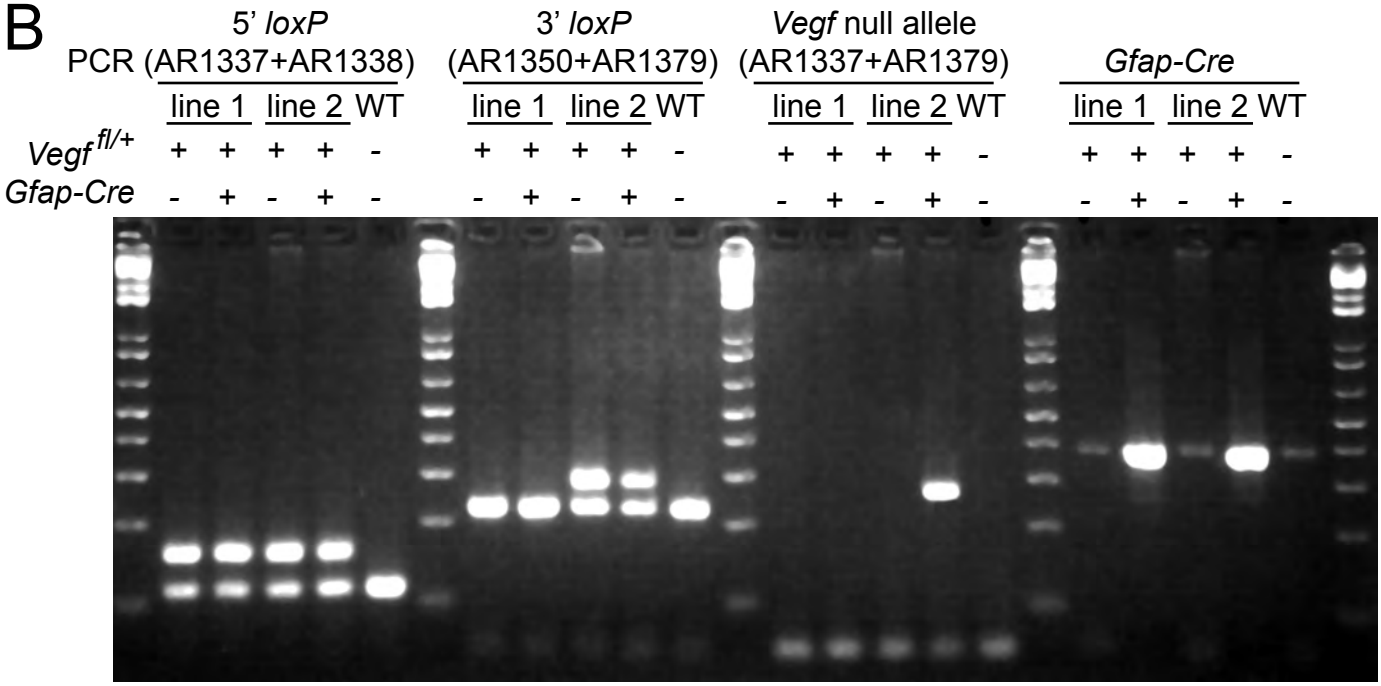

Rattner et al. Figure S7